Liquid Crystals
Publication details, including instructions for authors and subscription information:
http://www.informaworld.com/smpp/title~content=t713926090

Structural characterization of the new polymorphic mesophases formed by bent-core molecules

A. Eremin; I. Wirth; S. Diele; G. Pelzl; H. Schmalfuss; H. Kresse; H. Nádasi; K. Fodor-Csorba; E. Gács-Baitz; W. Weissflog

Online publication date: 11 November 2010

To cite this Article Eremin, A. , Wirth, I. , Diele, S. , Pelzl, G. , Schmalfuss, H. , Kresse, H. , Nádasi, H. , Fodor-Csorba, K. , Gács-Baitz, E. and Weissflog, W.(2002) 'Structural characterization of the new polymorphic mesophases formed by bent-core molecules', Liquid Crystals, 29: 6, 775 — 782
To link to this Article: DOI: 10.1080/02678290210136328
URL: http://dx.doi.org/10.1080/02678290210136328

LIQUID CRYSTALS, 2002, VOL. 29, NO. 6, 775–782

Taylor & Francis
Taylor & Francis Group

Structural characterization of the new polymorphic mesophases formed by bent-core molecules

A. EREMIN, I. WIRTH, S. DIELE, G. PELZL*, H. SCHMALFUSS, H. KRESSE, H. NÁDASI, K. FODOR-CSORBA†, E. GÁCS-BAITZ‡ and W. WEISSFLOG

Institut fur Physikalische Chemie, Martin-Luther-Universität Halle-Wittenberg, Mühlpforte 1, D-06108 Halle (Saale), Germany
†Research Institute for Solid State Physics and Optics of the Hungarian Academy of Sciences, Konkoly-Thege M. út 29-33, Budapest, Hungary
‡Chemical Research Center of the Hungarian Academy of Sciences, Institute of Chemistry, H-1525 Budapest, Hungary

(*Received 23 October 2001; in final form 25 January 2002; accepted 31 January 2002*)

A new achiral banana-shaped five-ring 2-methylresorcinol derivative fluorinated on the outer rings has been synthesized. This compound exhibits four antiferroelectric smectic phases characteristic for bent-core molecules (B_2, B_2', B_2'', B_5). In addition, a highly viscous solid-like phase has been detected which also shows electro-optical switching. This is the first switchable highly ordered B phase. The characterization of the mesophases was made by X-ray diffraction, electro-optical measurements and dielectric spectroscopy.

1. Introduction

Banana-shaped mesogens represent a new sub-field of thermotropic liquid crystals which attract not only great interest in the light of fundamental liquid crystal physics, but also with respect to possible practical applications. Because of the sterically induced polar packing of the bent molecules, new smectic-like mesophases can occur [1] which have no counterpart in calamitic liquid crystals. Up to now six new mesophases have been clearly identified, four of which exhibit ferro- or antiferro-electric properties [2]. The most frequently investigated phase is the so-called B_2 phase which possesses an antiferroelectric ground state and can be switched into ferroelectric states. Since the polar packed molecules are tilted with respect to the layer normal, the smectic layers possess C_2 symmetry. The combination of polar order and tilt leads to a chirality of the smectic layers although the individual molecules are achiral [3]. The B_5 phase is structurally quite similar to the B_2 phase; the only difference is an additional order of the central cores which still has short range order character [2, 4]. The B_1 phase is, in principle, a columnar phase, in which layer fragments of the B_2 phase form a rectangular two dimensional structure [2, 5]. In the B_6 phase the bent molecules are intercalated and tilted and corresponds to an intercalated B_2 structure [2, 6]. The structure of the B_7 phase is not yet known, but X-ray investigations on powder-like samples point to a 2D or 3D superstructure, although the lateral distances are liquid-like [7, 8]. The characteristic features of this phase are screw-like domains and unusual optical textures which indicate a helical superstructure [7, 8]. Recently we discovered a polar biaxial SmA phase where the banana-shaped molecules are packed in the bent direction, but in contrast to the B_2 phase they are arranged parallel to the layer normal [9]. The symmetry of this phase is C_{2v} and the equilibrium state is an antiferroelectric one. This smectic phase was theoretically predicted by Brand *et al.* [10] and designated C_P.

In this paper we present a new five-ring banana-shaped mesogen with a CH_3 group in the 2-position of the central core and with fluorine substituents at the terminal rings. Four mesophases could be clearly distinguished and characterized by X-ray investigations, by electro-optical measurements and by dielectric spectroscopy.

2. Material

The compound 2-methyl-1,3-phenylene bis[4-(3-fluoro-4-*n*-octyloxyphenyliminomethyl)benzoate] was prepared by reaction of 4-(3-fluoro-4-*n*-octyloxyphenyliminomethyl)-benzoic acid with 2-methylresorcinol using dicyclohexylcarbodiimide according to the procedure described in [11].

*Author for correspondence;
e-mail: schramme@chemie.uni-halle.de

Liquid Crystals ISSN 0267-8292 print/ISSN 1366-5855 online © 2002 Taylor & Francis Ltd
http://www.tandf.co.uk/journals
DOI: 10.1080/02678290210136328

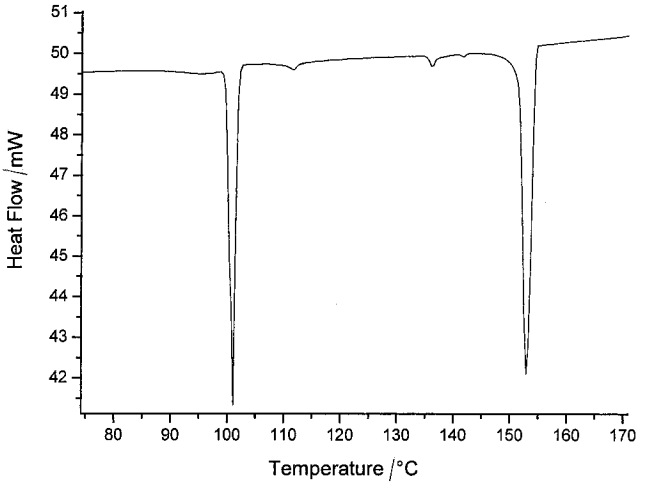

Figure 1. DSC thermogram (cooling run).

After recrystallization from DMF–ethanol (three-times) and toluene–heptane (twice) the yield was 23.5%.

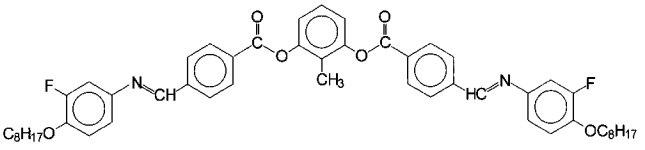

NMR (400 MHz, $CDCl_3$): $\delta = 0.86$–0.90 (m, 6H, CH_3), 1.24–1.51 (m, 20H, $(CH_2)_5$), 1.79–1.86 (m, 4H, $OCH_2C\underline{H}_2$), 2.13 (s, 3H, Ar–CH_3), 4.05 (t, $^3J = 6.6$ Hz, 4H, OCH_2), 6.98 (t, $^3J = 8.5$ Hz, 2H, Ar–H), 7.04–7.07 (m, $^3J = 8.5$ Hz, $^4J = 2.5$ Hz, 2H, Ar–H), 7.11 (dd, $^4J = 2.5$ Hz, 2H, Ar–H), 7.15 (d, $^3J = 8.1$ Hz, 2H, Ar–H), 7.32 (d, $^3J = 8.1$ Hz, 1H, Ar–H), 8.02 (d, $^3J = 8.4$ Hz, 4H, Ar–H), 8.30 (d, $^3J = 8.4$ Hz, 4H, Ar–H), 8.53 (s, 2H, CH=N)

The transition temperatures determined by differential scanning calorimetry (DSC) are related to the cooling run at a rate of 10 K min^{-1} (figure 1). In the transition scheme below the results of the phase assignments are presented. The numbers below the transition temperatures designate the transition enthalpies in kJ mol^{-1}.

$$\mathrm{I}\ \underset{[18.10]}{153^\circ\mathrm{C}}\ \mathrm{B_2}\ \underset{[\dagger]}{147^\circ\mathrm{C}}\ \mathrm{B_2'}\ \underset{[0.04]}{142^\circ\mathrm{C}}\ \mathrm{B_2''}\ \underset{[0.40]}{136^\circ\mathrm{C}}$$

$$\mathrm{B_5}\ \underset{[0.50]}{112^\circ\mathrm{C}}\ \mathrm{B_x}\ \underset{[11.40]}{103^\circ\mathrm{C}\ddagger}\ \mathrm{Cr}$$

3. Experimental

The phase transition temperatures were determined using a differential scanning calorimeter (DSC—Pyris 1, Perkin Elmer). The optical textures were observed using a polarizing microscope (Leitz Laborlux) equipped with a Linkam hot stage and an automatic temperature controller. X-ray diffraction (XRD) experiments on non-oriented samples were performed with a focusing Guinier goniometer (Huber Diffraktionstechnik, GmbH). Oriented samples were obtained by long annealing of a drop of the liquid crystal on a glass plate after slow cooling of the isotropic liquid. In this case the smectic layers are arranged parallel to the substrate. The X-ray patterns were obtained using a 2D detector (HI-Star, Siemens AG). Because of the special sample preparation, the lower part of the reciprocal sphere is shadowed. In order to estimate the intensity near the equator, the experimental curves $I_{meas}(\chi)$ were normalized with a transmission function $t(\chi)$, where χ is an angle between the scattering vector and the equator [9]. The transmission function $t(\chi)$ has been obtained by recording the scattering of the sample in the isotropic phase. In this ideal case the intensity of the diffuse scattering is independent of χ.

The electro-optical measurements were carried out using commercial ITO cells (EHC) of thickness 5 and 10 μm with and without rubbed polyimide layers. However, the surface treatment did not help to obtain uniformly oriented samples. The cells were filled with the liquid crystal in the isotropic phase and slowly cooled in the presence of a square-wave voltage (100 V, 50 Hz). The measurements were made employing the triangular-wave technique as well as the square-wave method where the voltage varies from 100 V to 0 V.

Dielectric measurements were performed in the frequency range from 1 Hz to 10 MHz using a Solartron Schlumberger SI 1260 impedance analyser and the Chelsea Interface. A brass cell coated with gold ($d = 0.05$ mm) was used as capacitor. The calibration was made with cyclohexane. It should be noted that all the measurements were performed on cooling the sample.

4. Results

4.1. *Polarizing microscopy*

The B_2 phase appears on cooling the isotropic liquid and exhibits a grainy fan-shaped texture, figure 2(*a*). At the transition $B_2 \rightarrow B_2'$ the texture does not change, whereas at the transition $B_2' \rightarrow B_2''$ a paramorphotic smooth fan-shaped texture arises, figure 2(*b*). The transition into the B_5 phase is accompanied by a minor change of the texture—by a small change of the birefringence and by the formation of irregular stripes perpendicular to the fans, figure 2(*c*). The transition into the low temperature phase B_X could not be recognized by polarizing microscopy.

†This transition was observed using NMR and XRD techniques and was not detected by DSC.

‡The melting point on heating is 125°C, meaning that the B_X phase is monotropic and occurs only on cooling the B_5 phase.

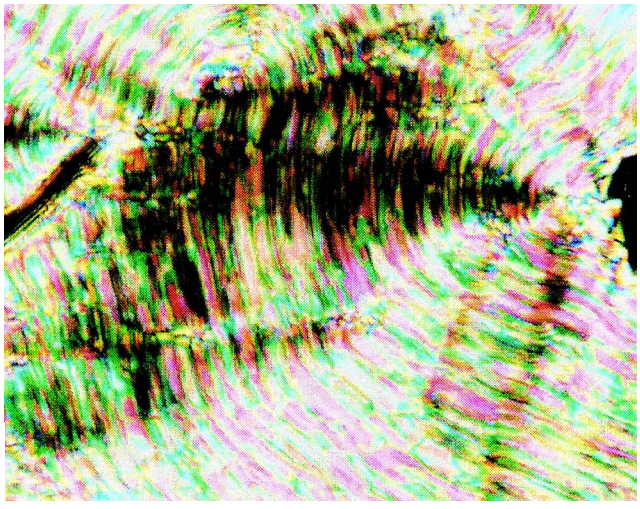

(a)

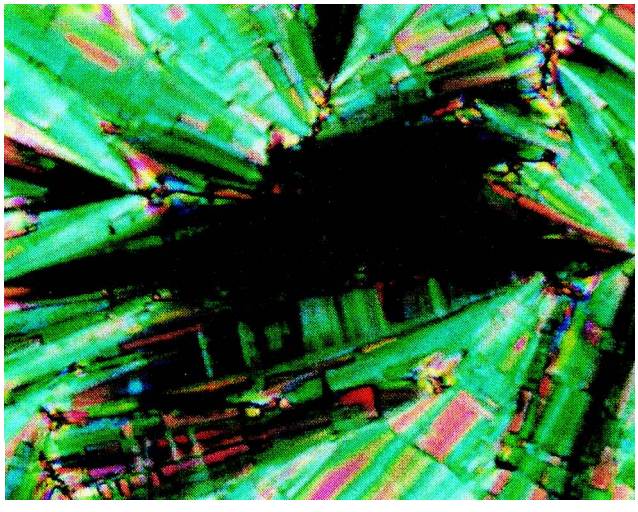

(b)

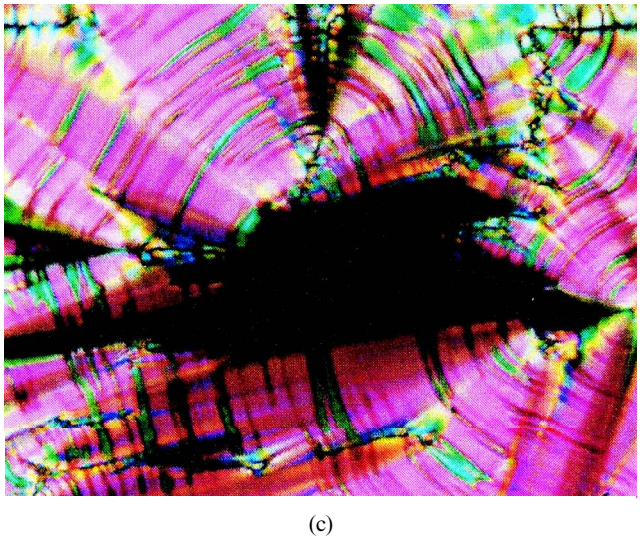

(c)

Figure 2. Optical textures of (*a*) the B_2 phase (148°C); (*b*) the B_2'' phase (140°C); (*c*) the B_5 phase (130°C).

With the exception of the phase transition $B_2 \rightarrow B_2'$, which has been observed in NMR and XRD experiments, all transitions have been detected by differential scanning calorimetry (figure 1). It is remarkable that the clearing enthalpy is higher than the melting enthalpy. On the other hand, the transition enthalpies between the B phases are rather low (0.04–0.5 kJ mol^{-1}).

4.2. *Electro-optical investigations*

All four phases showed similar electro-optical responses to the applied d.c. electric field. The initial fan-shaped texture transformed into a smooth SmA-like fan-shaped texture at a field higher than a threshold of 0.5–0.8 V μm^{-1} for the mesophases B_2, B_2', B_2'' and B_5 (figures 3 and 4). The textures relax into their initial state when the external field is removed (at $E = 0$).

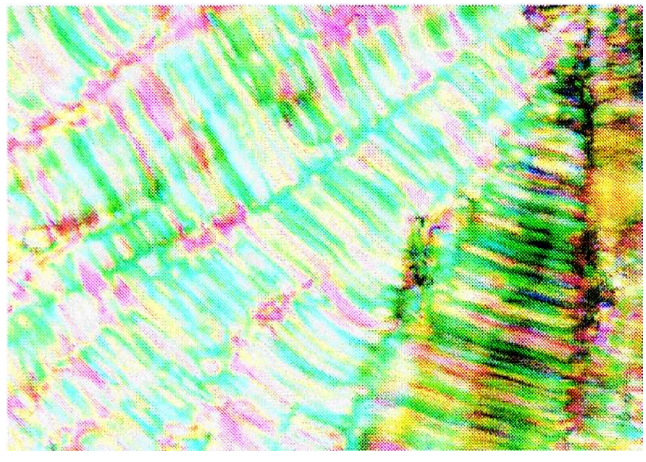

(a)

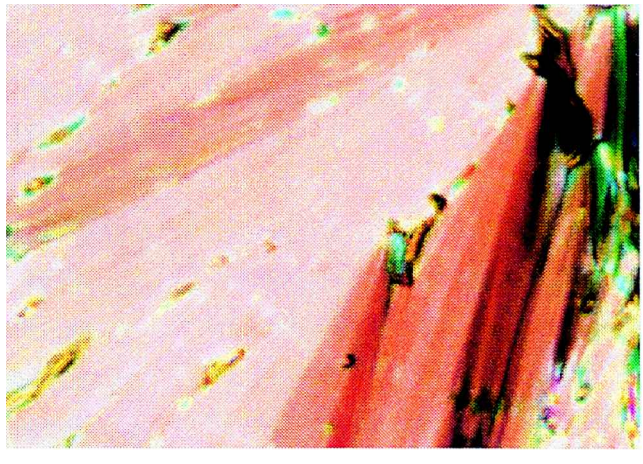

(b)

Figure 3. Field-induced texture change of the B_2' phase: (*a*) field-off state; (*b*) ± 2.8 V μm^{-1} (cell thickness 10 μm, temperature 143°C).

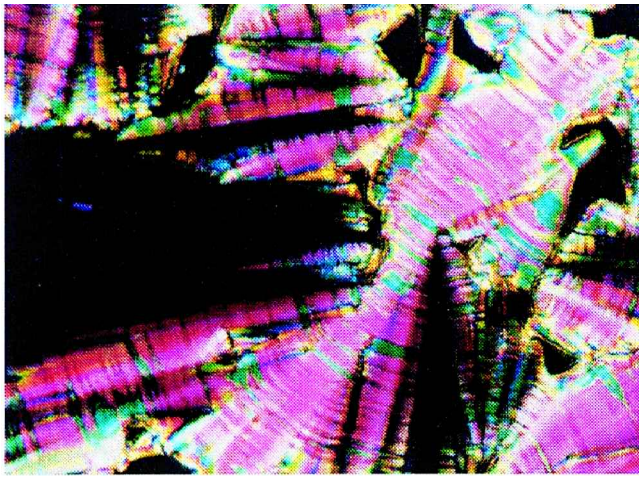

(a)

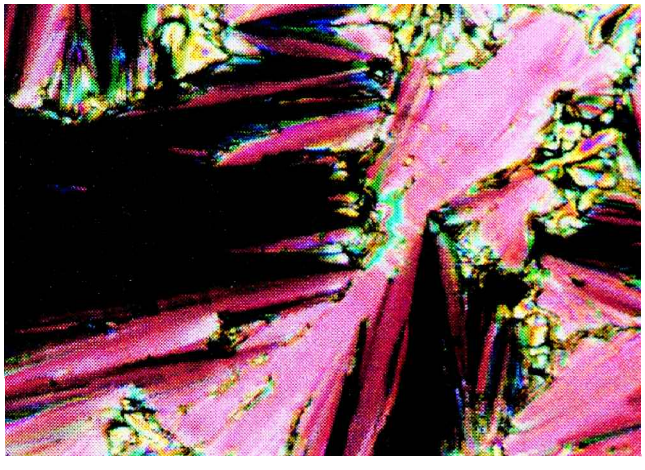

(b)

Figure 4. Field-induced texture change of the B_5 phase: (*a*) field-off state; (*b*) ± 4.8 V μm^{-1} (cell thickness 10 µm, temperature 132°C).

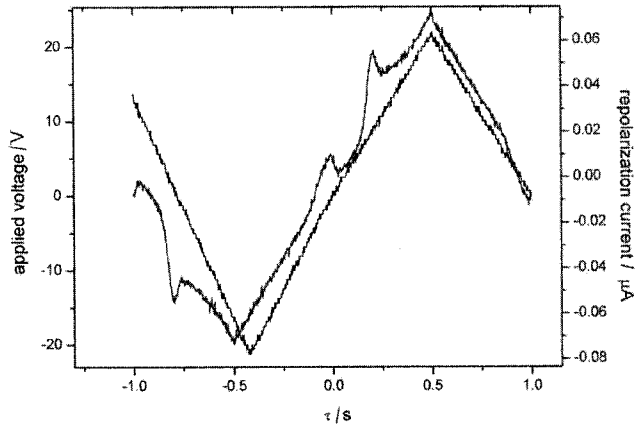

(a)

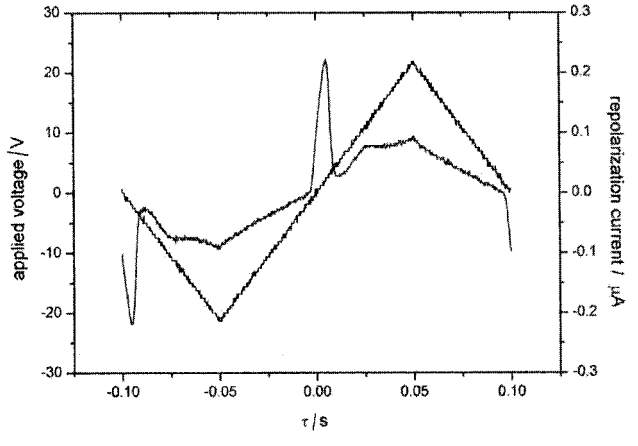

(b)

Figure 5. Switching current response of the B_2'' phase to an applied triangular wave field at $T = 141$°C: (*a*) $f = 0.5$ Hz, $E_{pp} = 4.0$ V μm^{-1}; (*b*) $f = 5$ Hz, $E_{pp} = 4.0$ V μm^{-1}.

The current response to the applied triangular-wave voltage contains two peaks of repolarization current, figure 5 (*a*). From this finding, together with the relaxation of the polarized state into the initial state in the experiments with d.c. voltage, we can assume an antiferroelectric (AFE) ground state of the mesophases. However the two current response peaks were observed at considerably low frequencies 1.0–0.5 Hz, and only one peak was observed at higher frequencies, figure 5 (*b*). The repolarization signals have also been observed on applying a square impulse varying from $E > E_{th}$ to $E = 0$. If the time of relaxation of the field-induced ferroelectric state (FE) into the AFE state is larger than the period of the applied field, a direct switching between two FE states occurs. In this case only one current peak appears. This phenomenon has been shown by Lee *et al.* [12] for the chiral antiferroelectric SmC_A^* phase where only one current response peak was observed at high frequencies. Recently, Bedel *et al.* [13] found a similar effect on 'banana' phases.

Figure 6 displays the temperature dependence of the spontaneous polarization, which reaches 800 nC cm^{-2}. At the transition into the low temperature phase B_X the threshold significantly increased. The relaxation from the polarized state into the ground state was quite slow, probably due to the high viscosity of the sample.

4.3. *X-ray investigations*

The XRD patterns of the three high temperature phases show equally spaced Bragg reflections indicating a layer structure. The layer spacing does not change markedly over the whole temperature range of these phases and is equal to 4.08–4.16 nm.

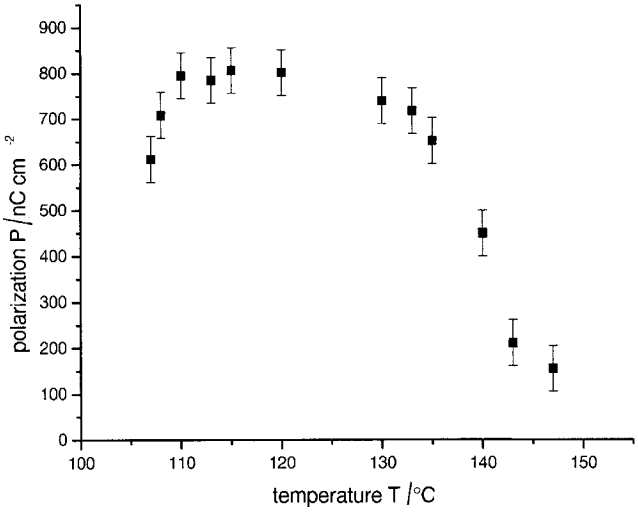

Figure 6. Temperature dependence of the spontaneous polarization.

The patterns of oriented samples display some further details (figure 7). The high temperature phase exhibits a pattern typical for a tilted smectic phase without in-plane order, like SmC or B_2 (the latter has been confirmed by the electro-optic technique): the layer reflections are observed on the meridian; the maxima of the broad outer diffuse scattering are situated out of the equator indicating an inclination of the molecules and the absence of long range positional order within the layers, figure 7(*a*). From the χ-scan the tilt angle of about 25° has been derived. On cooling the sample into the B_2' phase, the meridian reflections split up into pairs, as can be seen from the enlarged profile shown in the inset of figure 7(*b*). This splitting corresponds to an angle of ~6° between the layer normal and the fibre axis. This tilt is too small to be detected from the wide angle diffuse outer scattering. However, this change conforms with alterations in the NMR spectra. The split peaks merge again on the meridian at the transition into the B_2'' phase at 142°C. Below 135°C another mesophase appears where, in addition to the diffuse wide angle scattering, two stripes perpendicular to the equator are observed; see the equatorial scan in figure 7(*c*). The continuous stripes express the fact that there is no positional correlation between the molecules from different layers and the position of the stripes indicates positional ordering within the layers. The intensity profile along the stripe has a maximum on the equator as well as above and below it. Thus, the scattering diagram can be described by the formation of a two-dimensional

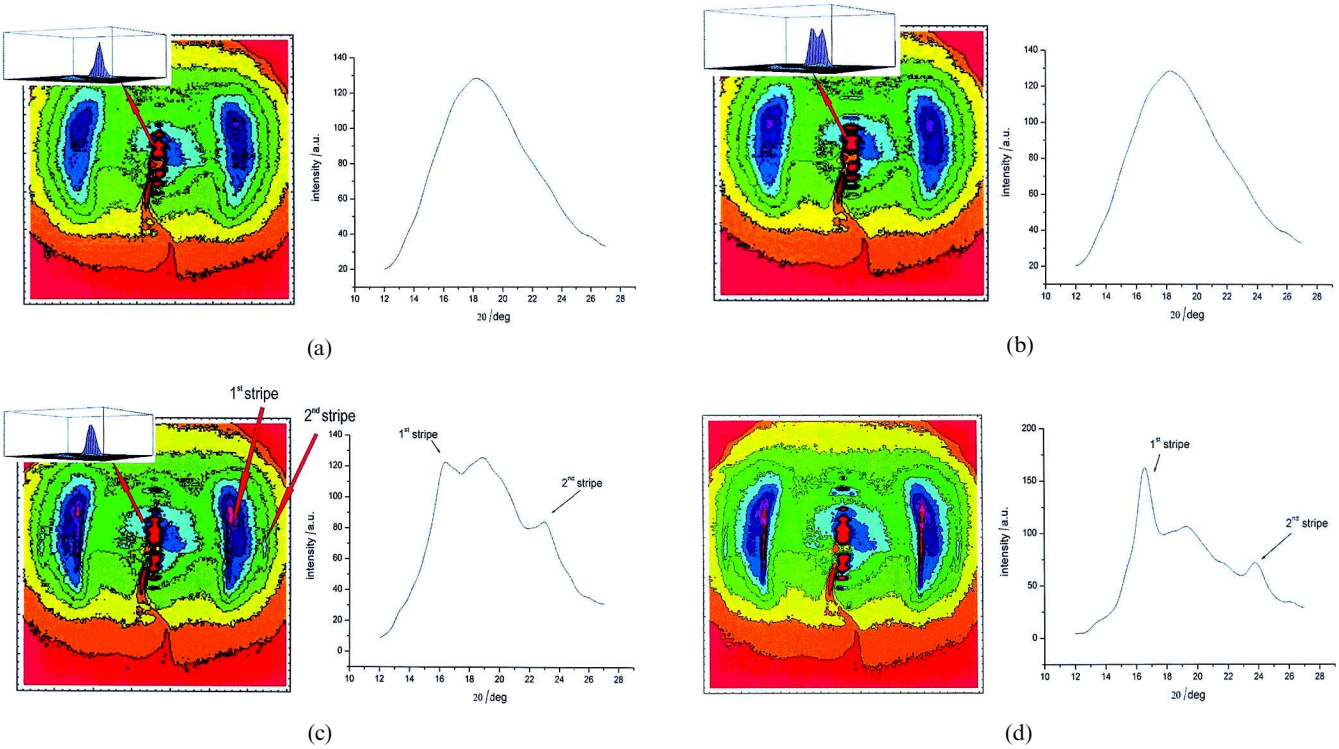

Figure 7. X-ray patterns of oriented samples and their equatorial intensity scans; the inset pictures show a three-dimensional profile of the meridian (0 0 1) reflection: (*a*) B_2 phase ($T = 149$°C); (*b*) B_2' phase ($T = 145$°C); (*c*) B_5 phase ($T = 120$°C); (*d*) B_X phase ($T = 110$°C).

rectangular cell within the layers on a short range scale, which is characteristic of a B_5 phase. With decreasing temperature, the intensity on the equator becomes more and more pronounced.

The pattern of the B_X phase is characterized by the appearance of distinct spots on the $h\,k$ rows, which indicates positional correlation of adjacent layers, figure 7(*d*). With respect to this, the phase can be considered as a three-dimensional crystal, although the remaining diffuse scattering implies a large amount of disorder in this phase. The position of the spots (perpendicular to the equator of the pattern) suggests an orthogonal cell. But some satellites around the $0\,0\,l$ reflections (out of the meridian) relate to a more complex structure (perhaps a helical superstructure), which cannot be resolved at present. The next change in the X-ray pattern takes place below $T \cong 102°C$. The scattering radiation condenses to many Bragg reflections corresponding to a true crystalline phase.

4.4. *Dielectric spectroscopy*

The experimental dependences of the real and the imaginary parts of the dielectric permittivity ε' and ε'' are given in figure 8. The processes of chemical decomposition, inevitable in such experiments, result in a slight decrease of the transition temperatures. Therefore, the temperature values had to be scaled to comply with the values obtained from other techniques (DSC, polarizing microscopy).

The experimental points for ε' and ε'' were fitted using the model described by equation (1) consisting of two Cole–Cole mechanisms (term 2 and 3), a conductivity

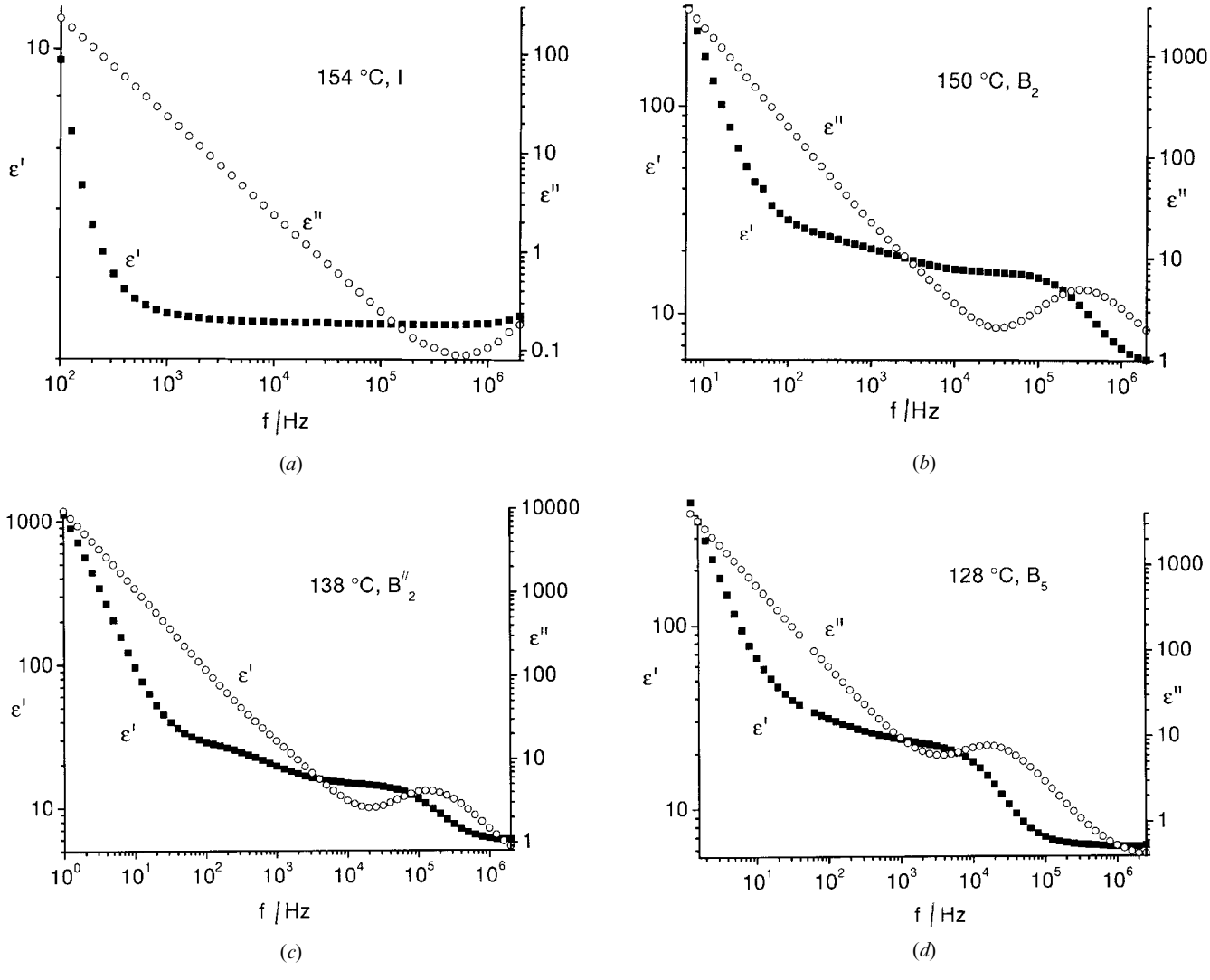

Figure 8. The real and imaginary part of the dielectric permittivity ($\varepsilon', \varepsilon''$) as a function of the frequency: (*a*) isotropic phase (154°C); (*b*) B_2 phase (150°C); (*c*) B_2'' phase (138°C); (*d*) B_5 phase (128°C).

contribution (term 4) and term 5 accounting for the capacitance of the ionic double layer appearing on the surface of the electrodes at low frequencies:

$$\varepsilon^* = \varepsilon_2 + \frac{\varepsilon_0 - \varepsilon_1}{1 + (\mathrm{i}\omega\tau_1)^{1-\alpha_1}} + \frac{\varepsilon_1 - \varepsilon_2}{1 + (\mathrm{i}\omega\tau_2)^{1-\alpha_2}} - \frac{\mathrm{i}A}{f^M} + \frac{B}{f^N} \quad (1)$$

where ε_i are the low and high frequency limits of the dielectric permittivity, $\omega = 2\pi f$ (f = frequency), τ_i are the relaxation times, α_i the Cole–Cole distribution parameters, the conductivity term is A ($\kappa = 2A\pi\varepsilon^0$, $\varepsilon^0 = 8.85 \times 10^{-12}$ As/Vm, if $M = 1$), and M, B and N are fit parameters responsible for the slope of the conductivity and capacity of the double layer.

The data acquired in the isotropic phase up to 50 kHz could be described well by use of the first and the last two terms. It is not necessary to consider a relaxation term since no dispersion of the dielectric permittivity was observed. Data at $f > 600$ kHz, which have been affected by the beginning of absorption at high frequencies and by a standing wave between the capacitor plates, were not used in fitting. In the B_2 phases, two absorption bands have to be taken into account for the data interpretation [14]. Thus, for the B_2 modifications a high frequency process at about 300 kHz and a low frequency one at 500 Hz, and for the B_2'' phase at 150 kHz and 300 Hz have been found; see figures 8(*b*) and 8(*c*), respectively. The limits of the dielectric permittivity calculated from the experimental data according to equation (1) are shown in figure 9. Confidence intervals for the dielectric permittivity given in equation (1) of $\Delta\varepsilon_0 = \pm 2.0$, $\Delta\varepsilon_1 = \pm 1$, $\Delta\varepsilon_2 = \pm 0.3$, as well as a relative error for the relaxation times τ_1 of $\pm 25\%$ and τ_2 of 10% were calculated. Since the error $\Delta\varepsilon_0$ increases with decreasing temperature, no data for ε_0 and τ_1 are given in figures 9 and 10 for temperatures below 136°C. The dielectric permittivity ε_1 reflects nearly all the phase transitions found by microscopic measurements and indicated by vertical lines. It should be noted that the dielectric increment $\Delta_2 = \varepsilon_1 - \varepsilon_2$ changes significantly at the I/B_2, B_2'/B_2'', and B_2''/B_5 transitions. A relatively high Δ_2 in the B phases in comparison with the isotropic liquid points to a strong positive dipole correlation. The decrease of Δ_2 at the B_5/B_X transition may be connected with either a complete disappearance or a stepwise decrease of the relaxation frequency of some decades (phase transition into a highly ordered solid-like B phase). The Cole–Cole distribution parameter was calculated to be $\alpha_2 = 0.01 \pm 0.01$ in all phases which corresponds to a classical Debye mechanism. For the low frequency absorption, Cole–Cole distribution parameters $\alpha_1 = 0.32 \pm 0.03$ (B_2) and 0.25 ± 0.03 (B_2') were obtained, pointing to a distribution of the relaxation times.

The relatively high value of $\varepsilon_2 = 6$ in the B_X phase indicates a modification in which fast dynamics of the polar end groups and probably also local motion within the core take place. This phase transforms at about 102°C slowly into a solid phase in which partial reorientation of dipoles occurs; therefore ε_2 decreases on further cooling to temperatures below 100°C to about 4 (not shown in figure 9).

The relaxation times are given in figure 10. Within error there is no difference between the data for τ_1 in phases B_2 and B_2'. A mean activation energy $E_A = (56 \pm 10)$ kJ mol^{-1} was calculated. We interpret this process as a collective motion of antiparallel ordered dipoles [15]. The faster process characterized by τ_2 is connected with the reorientation of the dipoles about

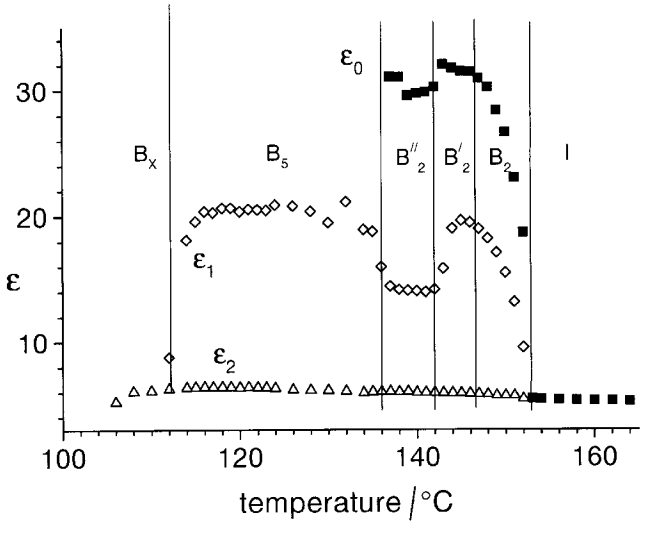

Figure 9. Limits of the dielectric permittivity in the isotropic, B_2, B_2', B_2'', B_5 and B_X phases.

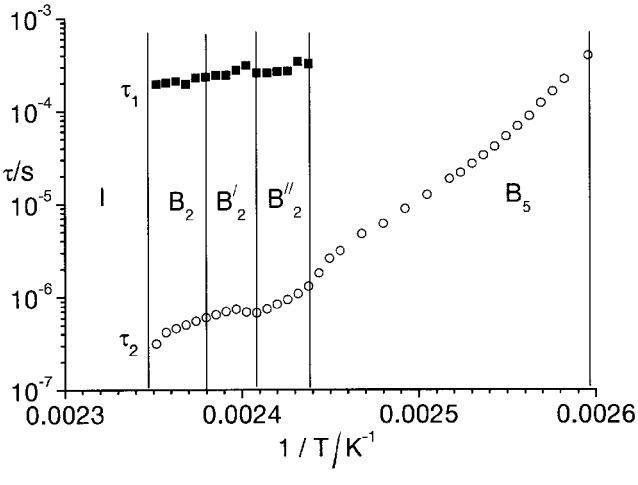

Figure 10. Relaxation times τ_1, τ_2 and their dependence on the inverse temperature in the B_2, B_2', B_2'' and B_5 phase.

the long axes. This process becomes partially one of collective character due to the strong steric interaction of the lateral dipoles among themselves [15]. The step in τ_2 at the B_2'/B_2'' transition is outside the experimental error. The decrease of the parameters Δ_2 and of τ_2 at the B_2'/B_2'' transition may indicate that in the B_2'' phase the interaction of the dipoles is reduced with respect to that in the B_2' phase and gives an argument for a phase transition. The mean activation energies $E_A(B_2) = (130 \pm 15)$ kJ mol^{-1}, $E_A(B_2') = (180 \pm 30)$ kJ mol^{-1} and $E_A(B_5) = (270 \pm 20)$ kJ mol^{-1} were calculated.

Discussion

In 1999 Ngyuen *et al.* [16] first reported bent-core mesogens with fluorine substituents on the outer rings. These compounds exhibited four tilted antiferroelectric smectic phases without in-plane order. However, no details about the structure of the mesophases were reported. In this paper we attempt to clarify the structural aspects of different switchable mesophases found in our compound.

The first high temperature phase appears as a tilted antiferroelectric phase with liquid-like order within the smectic layers. On the basis of our measurements employing XRD, NMR and dielectric spectroscopy we designate it as a B_2 phase. The transition into the B_2' phase is accompanied by splitting of the meridian reflections in the X-ray patterns of oriented samples; however, no extra reflections have been observed. The behaviour obtained from NMR spectroscopy (which will be discussed in a forthcoming paper) also indicates a phase transition. The results of the XRD measurements can by interpreted by a deformation or a breaking of the smectic layers, and the layer normal takes two directions with an angle $\sim 12°$ between them. A similar interpretation might be applied to our NMR results.

The splitting of the meridian reflections merges at $T = 142$°C, but they still remain quite broad. On the DSC diagram there is a small peak which corresponds to a phase transition. Clear evidence for this phase transition has been given by dielectric spectroscopy. The decrease of the relaxation time τ_2 and the decrease of the parameter Δ_2 found by the dielectric measurements indicate that in this phase the dipole interaction is reduced. In view of the similarity of the X-ray pattern of this phase and that of the B_2 phase, we call it B_2''.

The mesophase which arises on cooling the B_2'' phase could be identified as a B_5 phase. The additional diffuse scattering maxima on the equator of the X-ray pattern point to the continuous formation of positional order in the smectic layers, but the order is still restricted to the short range region. We were able to perform quantitative electro-optical investigations on the B_5 phase for the first time.

From the X-ray investigations it follows that the low temperature phase preliminarily designated as B_x is a three-dimensional solid-like phase. Surprisingly this phase shows electrical switching at sufficiently high electric field (10–20 V μm^{-1}). In contrast to the B_2, B_2', B_2'' and B_5 phases the switched state slowly relaxes to the ground state when the field is switched off. The B_x phase is the first switchable highly ordered 'banana phase'.

This work was supported by the Deutsche Forschungsgemeinschaft (DFG), the Fonds der Chemischen Industrie and DAAD.

References

[1] Niori, T., Sekine, T., Watanabe, J., Furukawa, T., and Takezoe, H., 1996, *J. mater. Chem.*, **6,** 1231.
[2] Pelzl, G., Diele, S., and Weissflog, W., 1999, *Adv. Mat.*, **11,** 707.
[3] Link, D. R., Natale, G., Shao, R., Maclennan, J. E., Clark, N. A., Körblova, E., and Walba, D. M., 1997, *Science*, **278,** 1924.
[4] Diele, S., Grande, S., Kruth, H., Lischka, Ch., Pelzl, G., Weissflog, W., and Wirth, I., 1998, *Ferroelectrics*, **212,** 169.
[5] Sekine, T., Niori, T., Sone, M., Watanabe, J., Choi, S. W., Takanishi, Y., and Takezoe, H., 1997, *Jpn. J. appl. Phys.*, **36,** 6455.
[6] Weissflog, W., Wirth, I., Diele, S., Pelzl, G., Schmalfuss, H., Schoss, T., and Würflinger, A., *Liq. Cryst.*, **28,** 1603.
[7] Pelzl, G., Diele, S., Jakli, A., Lischka, Ch., Wirth, I., and Weissflog, W., 1999, *Liq. Cryst.*, **26,** 135.
[8] Jakli, A., Lischka, Ch., Weissflog, W., Pelzl, G., and Saupe, A., 2000, *Liq. Cryst.*, **27,** 1405.
[9] Eremin, A., Diele, S., Pelzl, G., Nàdasi, Weissflog, W., Salfetnikova, J., and Kresse, H., 2001 *Phys. Rev. E*, **64,** 51 707.
[10] Brand, H. R., Cladis, P. E., and Pleiner, H., 1992, *Macromolecules*, **25,** 7223.
[11] Weissflog, W., Nàdasi, H., Dunemann, U., Pelzl, G., Diele, S., Eremin, A., and Kresse, H., 2001, *J. mater. Chem.*, **11,** 2748.
[12] Lee, J., Chandani, A. D. L., Itoh, K., Ouchi, Y., Takezoe, H., and Fukuda, A., 1990, *Jpn. J. appl. Phys.*, **29,** 1122.
[13] Bedel, J. P., Rouillon, J. C., Marcerou, J. P., Laguerre, M., Nguyen, H. T., and Achard, M. F., 2001, *Liq. Cryst.*, **28,** 1285.
[14] Schmalfuss, H., Hauser, A., and Kresse, H., 2000, *Mol. Cryst. liq. Cryst.*, **351,** 221.
[15] Hauser, A., Schmalfuss, H., and Kresse, H., 2000, *Liq. Cryst.*, **27,** 629.
[16] Nguyen, H. T., Rouillon, J. C., Marcerou, J. P., Bedel, J. R., Barois, P., and Sarmento, S., 1999, *Mol. Cryst. liq. Cryst.*, **328,** 177.